

Computation of Geodesic Voronoi Diagrams in Riemannian 3-Space using Medial Equations

Henning Naß, Prof. F.-E. Wolter, Hannes Thielhelm and Cem Doğan

Division of Computer Graphics

Institute for Men-Machine-Communication

Leibniz Universität Hannover, Germany

<http://gdv.uni-hannover.de>

nass@gdv.uni-hannover.de

fwolter@mit.edu

Abstract—The Voronoi diagram has been investigated intensively throughout the last decades. This has been done not only in the context of Euclidean geometry but also in curved spaces. Except for [KWR97] these methods typically make use of some fast marching cube algorithms. In this work we will focus on the computation of Voronoi diagrams including Voronoi objects that are contained in a Riemannian manifold M . Further, we assume throughout this paper that M has a differentiable structure consisting of smooth parametrisation functions $f_i, i \in I$. This is the reason why the approach presented in this work differs from the aforementioned algorithms. More accurate algorithms can be obtained by using to some medial equations that heavily involve normal coordinates. This approach relies on the precise computation of shortest joins of any two given points $, q \in M$. For these computations we did not apply shooting methods or related methods. Instead, we used a new perturbation method that operates on a family of deformed manifolds M_t , assuming that M_0 has constant sectional curvature. To reduce time and space complexity of the introduced algorithm we suggest to use a randomised incremental construction scheme (RICS). Our approach assumes that those points fulfil a general position requirement for computing the geodesic Voronoi diagram for a set of points. Finally results of some computed Voronoi diagrams will be presented.

I. INTRODUCTION

We assume that we have been given a complete Riemannian manifold M , which means that every two distinct points p and q in M can be joined by a length minimal arc length parametrised and smooth curve. This length can be regarded as the distance $d(p, q)$ of the points p and q . It can be shown that (M, d) is a metric space. Let $S = \{p_1, \dots, p_n\} \in M$ be the set of sites. Every site p_i can be related to its Voronoi region $VR(p_i, S)$ containing all points p that are closer to p_i than to any other site $p_j, j \neq i$.

The main innovative contribution of this paper is the introduction of local methods that for the first time make the precise computation of Voronoi diagrams of discrete point sets in 3-dimensional manifolds feasible in case the points fulfil a general position assumption and in case every Voronoi region is contained in a geodesically convex set. This means that any two distinct points can be joined by a unique geodesic being contained in the convex set.

The natural distance function d that makes M a metric space is essential for this definition of Voronoi regions. The Voronoi

diagram that is defined to be the complement of these regions thus consists of faces, edges and vertices under some regularity assumptions. Each vertex c corresponds to a circumsphere $S(c, r)$ being similarly defined as for the classical Euclidean Voronoi diagrams. The **circumsphere condition** says that the open ball $B(c, r) := \{p \in M; d(c, p) < r\}$ shall not contain any site p_i for all $i = 1, \dots, n$.

The randomised incremental construction scheme tries to compute the Voronoi diagram inside a symbolic sphere $S \subset M$ containing all relevant features of the Voronoi diagram. S can be seen as the bisector of every point p_i and the additional site ∞ . Therefore, the RICS begins with five sites $R = \{p, q, r, s, \infty\}$ and introduces the remaining sites $u \in S \setminus R$ step by step. It uses a history graph and a directed acyclic graph for its implementation. To reduce time complexity it only computes the skeleton of the updated Voronoi diagram in every step. The update of the skeleton leads to an intersection problem of the old Voronoi edges and the new Voronoi region $VR(u, R \cup \{u\})$, where R represents the sites that have already been introduced and u the site that is introduced next.

One main goal of this work is to introduce an algorithm that finds an initial vertex of the sites p, q, r, s for which we use different concepts. It will be assumed that every vertex of the Voronoi diagram $V(R)$, for $R \subset S$, lies on the intersection curve of two bisectors B_1, B_2 . We will sketch an idea of how to parametrise these intersection curves assuming we have an initial point x of this curve. The construction of x therefore will represent the main difficulty for the construction of the initial vertex.

The geodesic polar coordinates can be seen as a natural generalisation of the Euclidean polar coordinates. These polar coordinates involve the geodesic differential equations being a classical instrument of Riemannian geometry. As long as the sphere S is a convex neighbourhood of the sites S , it can be assured that the geodesic polar coordinates of a site provide a reparametrisation of M inside S . Under some more assumption we can assure that the geodesic Voronoi diagram has the same topological properties as the Euclidean Voronoi diagram. This will be the fundamental assumption of this work.

II. BASICS OF DIFFERENTIAL GEOMETRY AND VORONOI DIAGRAMS

Voronoi diagrams have been the focus of many researchers during the last decades and they gained much in importance in areas like theoretical physics, Geoinformation systems (GIS), medicine, mechanical engineering and so on. This list can be heavily extended but there is no intention to note all of them.

The definition of the Voronoi diagram, that is sometimes called the metric fundamental polygon, is rather simple. Think of a metric space (M, d) and some sites

$$S = \{p_1, \dots, p_n\} \subset M. \quad (1)$$

We are mainly interested in the situation where M is a complete Riemannian manifold and the sites only represent points. However the following approach does not need this specialised situation.

Definition 1: Given two sites $p, q \in M$, the **bisector** $B(p, q)$ consists of all points $x \in M$ that have the same distance to p as to q , i.e.

$$B(p, q) = \{x \in M | d(p, x) = d(q, x)\}. \quad (2)$$

In addition the metric d makes it possible to define **half spaces** as in the Euclidean case.

Definition 2: Let $p, q \in M$. $D(p, q)$ is the set of all points that are closer to p than to q :

$$D(p, q) = \{x \in M | d(p, x) < d(q, x)\} \quad (3)$$

A analogue characterisation can be made for q :

$$D(q, p) = \{x \in M | d(p, x) > d(q, x)\} \quad (4)$$

Now it is possible to declare Voronoi regions and the Voronoi Diagram:

Definition 3:

$$VR(p, S) = \bigcap_{q \in S \setminus \{p\}} D(p, q) \quad (5)$$

is called **Voronoi region** of p with respect to S . Furthermore

$$V(S) = \bigcup_{p \in S} \partial VR(p, S) \quad (6)$$

is titled **Voronoi diagram** of the reference set S .

The geometry of Euclidean Voronoi diagrams has been investigated for ages and it is known that the Voronoi regions are convex having polygonal boundaries. In fact not all metrics d give rise to meaningful Voronoi diagrams but luckily there are only few of them. The Manhattan metric for example causes bisectors that may look strange in case the site p and q are diagonal vertices of a square.

Now and in the following M is a complete Riemannian manifold with induced metric d . Later on we will specialise to manifolds that are hypersurfaces $M \subset \mathbb{R}^{n+1}$. A **graph manifold** M for example is characterised by the fact that for the description of M only one smooth height function h is required:

$$M = \{(x_1, \dots, x_4) \in \mathbb{R}^4 | x_4 = h(x_1, x_2, x_3)\}. \quad (7)$$

There is an advantage to concentrate only on this simple case because it yields an easier implementation of the randomised incremental construction scheme. Yet the algorithm involves the determination of the shortest joins of two points p and q on the hypersurface. In case the underlying manifold can be parametrised by one parametrisation function (or implicit function) we were able to derive an efficient algorithm for the shortest path problem using some very simple perturbation arguments as described later on. We also made computations on manifolds for which there exists a radius function

$$r : S_3 \rightarrow \mathbb{R}_{\geq 0} \quad (8)$$

such that every point $p \in M$ has the Cartesian coordinates

$$p = r(y)y,$$

where y denotes the local parametrisation of the sphere S_3 . The first fundamental tensor (g_{ij}) that measures for example the length of curves on such hypersurfaces has diagonal form, if the standard spherical coordinates are used.

There are some important properties of geodesic Voronoi diagrams that need to be mentioned. Useful is the following definition of convex sets.

Definition 4: A set $C \subset M$ is called **strong convex** if and only if for every two points $p, q \in C$ every shortest geodesic between p and q belongs to C . We say that C is **weakly convex** if there exists at least one shortest geodesic joining p and q that completely lies in C .

Note that singletons are always strongly convex. The generalisation of star shaped sets is important for some properties of Voronoi regions.

Definition 5: A set $C \subset M$ is called **strongly star shaped** if and only if there exists a centre point $p \in C$ such that for every point $q \in C$ every shortest geodesic between p and q belongs to C . C is **weakly star shaped** if for every $q \in C$ there is at least one shortest geodesic between p and q that lies in C .

This yields the following

Theorem 1: Consider a complete and connected Riemannian manifold M with intrinsic distance function d . Every Voronoi region $VR(p, S)$ is strong star shaped with centre p .

Proof: Let $x \in VR(p, S)$. Assume there is a shortest geodesic $\gamma : [0, s] \rightarrow M$ with $\gamma(0) = p$ and $\gamma(s) = x$ and $y = \gamma(t) \notin VR(p, S)$. This means that y belongs to a Voronoi region of another point $q \in S$ or to the bisector $B(p, q)$. In either cases we have $d(p, y) \geq d(q, y)$. As a result

$$\begin{aligned} d(p, x) &= d(p, y) + d(y, x) \\ &\geq d(q, y) + d(y, x) \\ &\geq d(q, x). \end{aligned}$$

This is contradictory to the assumption that x belongs to the Voronoi region $VR(p, S)$. Thus, the proof is complete. ■

A direct consequence of this theorem is the next

Corollary 1: Let M a complete and connected Riemannian manifold and d the Riemannian distance function. Every Voronoi region is connected.

Theorem 2: Let (M, d) a metric space and S the set of sites. Then every Voronoi region $VR(p_i, S)$ is open and $V(S)$ is closed.

Proof: It suffices to show that every half space $D(p, q)$ for distinct p and q is open. Let $x \in D(p, q)$. From the definition of the half space we get $d(p, x) < d(q, x)$. Assume that for every $r > 0$ there exists an $y_r \in B_r(x)$ with larger distance to p than to q . Consider the sequence $r_n = 1/n$. Conclude that

$$d(p, y_{r_n}) \geq d(q, y_{r_n}), \quad (9)$$

$$d(x, y_{r_n}) \rightarrow 0. \quad (10)$$

Taking the limits it turns out that x did not belong to the half space $D(p, q)$ since $d(p, x) \geq d(q, x)$ as a direct consequence from (9) and (10). $V(S)$ is the complement of the open set

$$\bigcup_{i=1}^n VR(p_i, S)$$

and thus closed. \blacksquare

The construction of the geodesic Voronoi diagram may be very time-consuming and it is not a priori clear, if there is an affinity between the Euclidean Voronoi diagram and the geodesic Voronoi diagram. Let for example M be a two-dimensional Monge surface. Even if the induced metric d_M is equivalent to the Euclidean metric d_2 , i.e.

$$kd_2(x, y) \leq d_M(x, y) \leq Kd_2(x, y) \quad (11)$$

for $0 < k \leq K$, then there is no guarantee that even the bisector of two points is homeomorphic to a line.

Definition 6: Let S, M be Riemannian manifolds such that S is a submanifold of M . S is called **totally geodesic**, if every geodesic in S is a geodesic in M . In other words, the second fundamental form of S is zero.

Beem showed the following result for Pseudo-Riemannian manifolds (cf. [Bee75]):

Theorem 3: Let M be a Pseudo-Riemannian manifold and p, q points with nonzero distance. $B(p, q)$ is a totally geodesic submanifold if and only if M has constant curvature.

This means that under the circumstance $\dim(M) = 2$ and constant Gaussian curvature K every bisector is a geodesic. In fact, these cases are only of minor interest in the context of computational geometry. Nevertheless, it is an interesting result that we have a sufficient and necessary condition for bisectors being totally geodesic submanifolds. A nice classification of bisectors in a clearly arranged situation was done by Wolter (cf. [Wol85]).

The distance function mentioned several times before requires a few more explanations. It follows the concept of **geodesics** in a straight way which is often used in Riemannian geometry.

Definition 7: Let I be an interval and $\gamma : [a, b] \rightarrow M$ a differentiable curve. γ is called a **geodesic**, if the covariant derivative of the tangent $\dot{\gamma}$ vanishes everywhere, i.e.

$$\frac{D}{ds} \dot{\gamma}(s) = 0. \quad (12)$$

Every sufficiently small sub arc of a geodesic yields a shortest path of the corresponding end points. The covariant derivative generalises the concepts of directional derivatives from classical analysis guaranteeing the derivatives of vector fields is defined with respect to the Riemannian structure only, and therefore being independent of some special local coordinates. In case the Riemannian manifold is embedded into the Euclidean space the covariant derivative can be obtained by projection of the classical derivative onto the corresponding tangent plane (space). For more details we refer to [doC92]. It is similar to the directional derivative, however it involves a projection onto tangent spaces. It is known from the theorem of Hopf and Rinow that in complete Riemannian manifolds every two distinct points p and q can be joined by a distance minimal curve that is a geodesic. The uniqueness of such a geodesic is never guaranteed except for the case M is simply connected and has non positive sectional curvature. Employing some local parametrisation f of M , the equations

$$f((x_1(s), \dots, x_n(s)) = \gamma(s) \quad (13)$$

must hold with x_k fulfilling the geodesic equations

$$\ddot{x}_k(s) + \Gamma_{ij}^k \dot{x}_i(s) \dot{x}_j(s) = 0. \quad (14)$$

A geodesic is completely determined by the initial point and the initial direction because the geodesic equations build up a linear system of ordinary differential equations of order two.

The **offset function** \mathcal{O}_p of a point $p \in M$ can now be derived from the above notion of geodesics. Assume we have an orthonormal basis $\{e_1, \dots, e_n\}$ of the tangent space $T_p M$ of the point p . Let $s \geq 0$ and $v \in S_{n-1}$. There is a unique geodesic γ with initial conditions

$$\gamma(0, v) = p, \quad (15)$$

$$\dot{\gamma}(0, v) = \sum_{i=1}^n v_i e_i. \quad (16)$$

The offset function is then implicitly defined by

$$f(\mathcal{O}_p(s, v)) = \gamma(s, v), \quad (17)$$

where γ is the geodesic defined by the initial conditions from (15) and (16). The coordinates (s, v_1, \dots, v_{n-1}) are sometimes called **normal coordinates** of $\gamma(s, v)$ with respect to the point p . The **exponential map** can now be defined as follows. Let $v \in T_p M$ and $\gamma : [0, 1] \rightarrow M$ a geodesic with $\gamma(0) = p$ and $\dot{\gamma}(0) = v$, then $\exp_p(v) = \gamma(1)$. \exp operates on the tangent space $T_p M$ without further restrictions in case M is complete.

Finally a note on medial equations is given and in addition a extended definition of offset functions not only for points but also for curves or in general topological submanifolds.

Definition 8: Let A and B be two **progenitor objects**, $A, B \subset M$ with locally defined offset functions $\mathcal{O}_A(s, t_A)$ and $\mathcal{O}_B(s, t_B)$. Let $b : U \rightarrow \mathbb{R}$ a function and $\sigma_A, \sigma_B = \pm 1$. Define the system function

$$F(s, t_A, t_B) = \mathcal{O}_A(\sigma_A s, t_A) - \mathcal{O}_B(\sigma_B b(t_A) s, t_B) \quad (18)$$

The zeros of F are called **local medial set** and the system $F = 0$ **medial equations**.

III. THE SHORTEST DISTANCE PROBLEM

Let $p = f(x_p), q = f(x_q) \in M$. Our goal is to find s_0 and $v_0 \in S_{n-1}$ such that

$$\mathcal{O}_p(s_0, v_0) = x_q. \quad (19)$$

holds. This automatically leads to a boundary value problem for which several solution techniques have been established. The shooting method is a famous representative of this group of methods, but in fact, it lacks a systematic way of finding the solution, since it often uses Newton methods and generalised bisection techniques for the computation of the solutions.

Recall that M is a graph manifold of dimension three and \mathcal{O}_p is the offset function of the point p . Consider the family of graph manifolds

$$M_t = \{(x_1, \dots, x_4), x_4 = t \cdot h(x_1, x_2, x_3)\} \quad t \in [0, 1]. \quad (20)$$

Every M_t is a **graph manifold** and the set M_1 corresponds to the original manifold M .

Up to now we have only considered the offset function of a point being contained on a three-dimensional manifold M . The definition of the offset function can be extended to the family of manifolds M_t with respect to a parameter point $x_p \in \mathbb{R}^3$. Three parameters will be required for the definition: the parameter s that corresponds to the run length parameter of the geodesic, an initial direction v and the time parameter t . Since we refer to a family of manifolds it must be specified to which of these manifolds we will refer. For fixed time parameter t we obtain two maps given by

$$\begin{aligned} \pi_t : \begin{cases} M_t & \rightarrow \mathbb{R}^3 \\ p^t = (x_p, th(x_p)) & \mapsto x_p \end{cases} \\ \omega_t : \begin{cases} \mathbb{R}^3 & \rightarrow T_{p^t} M_t \\ v = & \mapsto \sum_{i=1}^3 v^i f_i^t \end{cases}, \end{aligned}$$

where f_i^t denotes the partial derivative $\frac{\partial}{\partial x_i} f^t$ of the parametrisation function

$$f^t(x_1, x_2, x_3) = \begin{pmatrix} x_1 \\ x_2 \\ x_3 \\ th(x_1, x_2, x_3) \end{pmatrix}.$$

This yields now the following definition of the offset function

$$f^t(\mathcal{O}_{x_p}(s, v, t)) = \exp_{\pi_t^{-1}(x_p)}(\omega_t(v)).$$

Note that $\mathcal{O}_{x_p}(s, v, t)$ is an implicitly and well defined function. Subject of the next considerations will be the implicit parametrisation of the zero set of the function defined by

$$F(t, v) = \mathcal{O}_{x_p}(t, 1, v) - x_q. \quad (21)$$

Straightforward considerations provide that $F(w_0) = 0$ in case $w_0 = (0, x_q - x_p)$. Now we can reformulate the given boundary value problem (BVP) as a family of initial value problems (IVP). If the Jacobian of the function F has full rank

in w_0 , the implicit function theorem states that there exist an $\epsilon > 0$ and a function $\rho : [0, \epsilon] \rightarrow \mathbb{R}^4$ such that

$$F(\rho(\tau)) = 0.$$

Thus, after implicit differentiation with respect to τ and normalisation we obtain the system

$$DF|_{\rho(\tau)} \cdot \rho'(t) = 0, \quad (22)$$

$$\langle \rho'(\tau), \rho'(\tau) \rangle = 1. \quad (23)$$

$F(0, v) = x_p - x_q + v$ finally proves that the implicit function theorem can in fact be applied. The Jacobi matrix of F is the crucial factor of our computations. It involves the solution of the geodesic equations and the Jacobi equations, which build up an important instrument in classical Riemannian geometry. We refer to [doC92] for further details. The hardest part of the computations is the determination of the partial derivative of \mathcal{O}_{x_p} with respect to the time parameter t . In most cases it is sufficient to approximate them by finite differences. It is then possible to improve the result for $t = 1$, employing some Newton method or related methods.

Figure 1 gives an impression of a trajectory $\tau \rightarrow v(\tau)$ for two parameter points $x_p = (1, 2, 3)$ and $x_q = (0, 1, -2)$ with metric induced by the height function $h = x^2 + y^2 + \sin(z)$. We finally get $d(p, q) = 5.1962\dots$ The unique arc length parametrised shortest geodesic that joins p and q has initial direction $\dot{\gamma}(0) = (-0.1900, -0.2398, -0.6850, -0.6612)$. For the error we get

$$\|\mathcal{O}_{x_p}(s_{\text{end}}, v_{\text{end}}) - x_q\| \leq 0.5 \cdot 10^{-8},$$

which means that the endpoint of the geodesic is very close to q and the application of the Newton method can reduce this error even more.

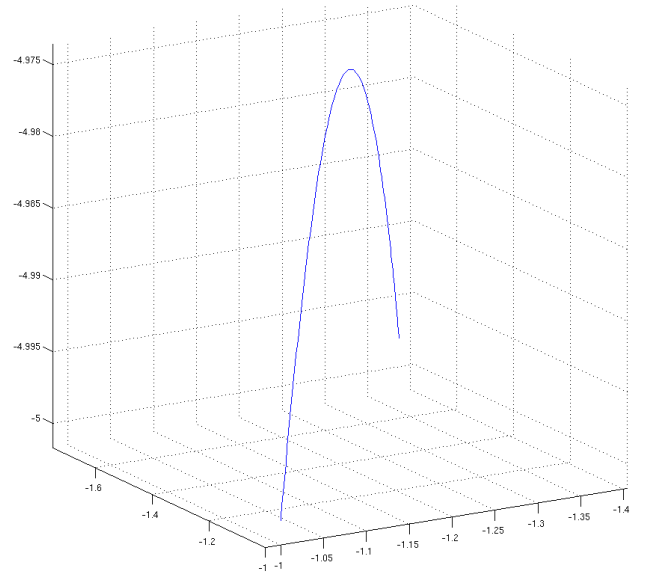


Fig. 1. Trajectory of the initial direction $\tau \rightarrow v(\tau)$

Note that for the manifolds defined by (8) the homotopy

$$r(y, t) = t \cdot r(y) + 1 - t \quad (24)$$

yields a differentiable deformation of a topological sphere

$$M_t = \{r(y, t)y; y \in S_3\},$$

recalling that M_0 is the sphere S_3 , for which geodesics are known explicit. y denote the standard spherical coordinates of a unit sphere. Details will be omitted here, since the definition of the offset function \mathcal{O}_{x_p} and the system function F are formally the same in both cases.

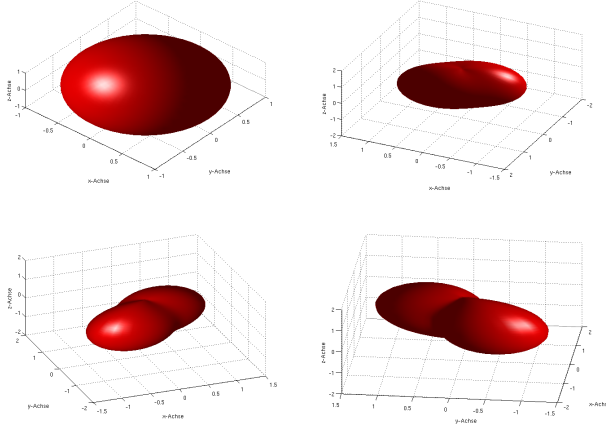


Fig. 2. Evolution of the deformation of a sphere

IV. DISTANCE SPHERES, VORONOI EDGES AND BISECTORS

Let M a 3-dimensional hypersurface. We present a generalisation of the property of points to be in general position.

Definition 9: Let $p_1, \dots, p_4 \in M$ be four points. The p_i are said to be in **general position** if there exists a distance sphere $S(c, r) = \{x \in M; d(x, c) = r\}$ with $p_i \in S(c, r)$ for all $i = 1, \dots, 4$.

The question if there could exist more than one distance sphere containing the four given points is answered by the next example.

Example 1: Let $M_a = \{(x, y, z); z = a(x^2 + y^2)\}$ be a paraboloid and $p_1 = (1, \epsilon, a(1 + \epsilon^2))$, $p_2 = (0, 0, 0)$, $p_3 = (1, -\epsilon, a(1 + \epsilon^2))$ for a sufficiently small $\epsilon > 0$. The projection of the Voronoi diagram $V(p_1, p_2, p_3)$ onto the xy -plane is for sufficiently large $a \gg 1$ homoeomorph to:

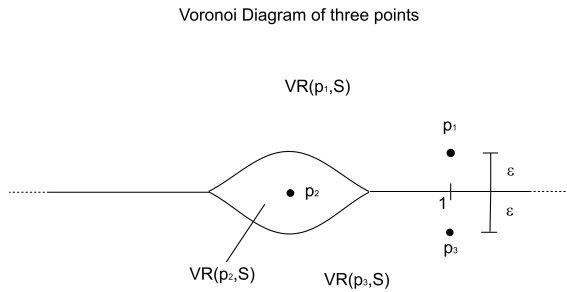


Fig. 3. Three points with 2 distance spheres

This can be seen from different reasons. The closure of the Voronoi region of the point p_2 is a compact set for sufficiently large a , since every point $p = (p_1, p_2, p_3) \in M_a$ with $p_3 \geq a(1 + \epsilon^2)$ is closer to p_1 and p_3 respectively. To proof this we build the intersection S of the plane $\{z = a(1 + \epsilon^2)\}$ with M_a . It is straightforward to see that S is a circle containing both p_1 and p_3 . The radius of this circle remains constant, in case a increases. The Riemannian distance from p_1 to any of the points on this circle can be bounded by a number $K > 0$. Note that K does not depend on a . The same is true for the point p_3 . The distance from p_2 to any of these points can be bounded from below by $a(1 + \epsilon^2)$, which tends to infinity, if a tends to infinity. Thus, the closure of the Voronoi region must be a compact set.

We now must show that the Voronoi diagram has two vertices. Therefore, consider the bisector $B(p_1, p_3)$ of the sites p_1 and p_3 . Simple arguments provide that

$$B(p_1, p_3) = \{(x, 0, ax^2); x \in \mathbb{R}\}.$$

Let $f(p) = d(p_2, p) - d(p_1, p)$, $p \in B(p_1, p_3)$. It can be proven that f has exactly two zeros. Every point $p = (p_1, p_2, p_3)$ with $p_2 > 0$ is closer to p_1 than to p_2 and hence cannot be a vertex. Similar arguments can be applied for points $p_2 < 0$. This completes the proof.

The last example showed that it cannot be guaranteed in every case that a geodesic Voronoi diagram has the same properties like the corresponding Voronoi diagrams in the Euclidean case. However, the uniqueness of the distance spheres can be ensured if for every site the Voronoi region of this site is properly contained in a convex set.

The computational aspects of finding the centre and the radius of such spheres should be explained at this stage. The geometry of these distance spheres may look strange as one can see by the next figure, displaying a distance sphere in the parameter space of a 3-dimensional Riemannian manifold.

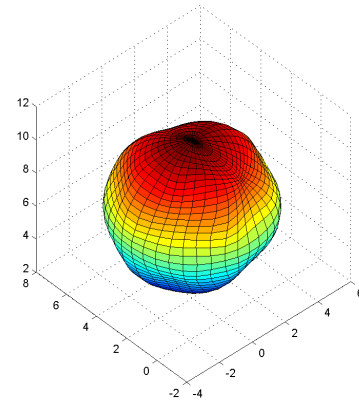


Fig. 4. Example of a distance sphere

Assume there exists a **normal neighbourhood** $U \subset M$ of all the sites p_1, \dots, p_n . A normal neighbourhood U of a point

p is characterised by the fact, that the exponential function

$$\exp_p : \exp_p^{-1}(U) \subset T_p M \rightarrow U$$

is invertible. We will even more assume that this neighbourhood contains all important features of the unbounded Voronoi diagram $V(S)$ that is discussed later on.

The main idea of how to find $S(c, r)$ is to trace the curve

$$B(p_1, p_2, p_3) = B(p_1, p_3) \cap B(p_2, p_3) \quad (25)$$

that will correspond to a Voronoi edge in case the distance sphere $S(c, r)$ does not contain any other point of $S = \{p_1, \dots, p_n\}$ but p_1, \dots, p_4 . This curve meets the centre after some time if it is tracked in both directions. An initial point of this curve is therefore required as well.

In order to find this initial point we will focus on the results of the last section. The unique arc length parametrised geodesic join $s \mapsto \gamma(s, v_1^0)$, $s \in [0, d(p_1, p_3)]$ between p_1 and p_3 can be obtained with these results. The midpoint of this curve, namely

$$m = \gamma\left(\frac{d(p_1, p_3)}{2}, v_1^0\right). \quad (26)$$

is supposed to be contained in the bisector $B(p_1, p_3)$. Set $s^0 = d(p_1, p_3)$. Now suppose the inverse image of $B(p_1, p_2, p_3)$ with respect to the local parametrisation f intersects with the unique plane P that contains the points $f^{-1}(m)$, $f^{-1}(p_2)$ and $f^{-1}(p_3)$. This plane is given in implicit representation

$$P : \langle a, x \rangle = a_1 x_1 + a_2 x_2 + a_3 x_3 = b. \quad (27)$$

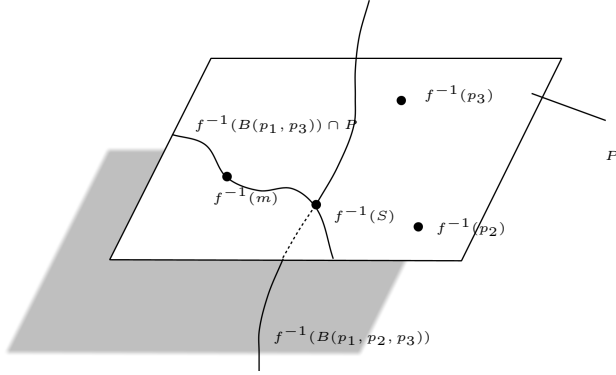


Fig. 5. Bisector intersection with the plane P

The intersection point $S = B(p_1, p_2, p_3) \cap P$ lies on the intersection curve

$$B(p_1, p_3) \cap P \quad (28)$$

for which we already have an initial point (here m). The system function for the intersection problem is defined as

$$F(s, v_1, v_3) = \begin{pmatrix} \mathcal{O}_{p_1}(s, v_1) - \mathcal{O}_{p_3}(s, v_3) \\ \langle a, \mathcal{O}_{p_1}(s, v_1) \rangle - b \\ \|v_1\|^2 - 1 \\ \|v_3\|^2 - 1 \end{pmatrix}. \quad (29)$$

If $s \mapsto \bar{\gamma}(s, v_3^0)$, $s \in [0, d(p_1, p_3)]$ denotes the unique arc length parametrised geodesic from p_3 to p_1 , which yields the same orbit like γ however having opposite orientation, it can easily be seen, that the direction v_3^0 can be obtained from the direction $\dot{\gamma}(s^0, v_1^0)$ and the orthonormal basis of $T_{p_3} M$.

In case of transverse intersection of $B(p_1, p_3)$ and $f(P)$ one can presume that there is a sufficiently large $\epsilon > 0$ and a function $\delta : [-\epsilon, \epsilon] \rightarrow \mathbb{R}^7$ such that $F(\delta(t)) = 0$ holds for all $t \in [-\epsilon, \epsilon]$ and in addition $\delta(0) = (s^0, v_1^0, v_3^0)$. A closer look at the system matrix DF yields

$$DF = \begin{pmatrix} \frac{\partial_s(\mathcal{O}_{p_1} - \mathcal{O}_{p_3})}{a^T \partial_s \mathcal{O}_{p_1}} & \frac{D_{v_1} \mathcal{O}_{p_1}}{a^T D_{v_1} \mathcal{O}_{p_1}} & \frac{-D_{v_3} \mathcal{O}_{p_3}}{0} \\ 0 & 2v_1^T & 0 \\ 0 & 0 & 2v_3^T \end{pmatrix}.$$

In fact for moderate fundamental tensors the constraints for the arc length parametrisation have no effect on the solution process or in other words it is decoupled from it. It is required that the bisectors intersect transversely. This is assumed to be true in a **convex neighbourhood** of the sites S .

Definition 10: A convex neighbourhood U of a point p is an open set $U \subset M$ containing p such that for every $x, y \in U$ there exist an unique geodesic joining x and y in U .

Now we have an initial point of the curve $B(p_1, p_2, p_3)$ and as stated before it will pass the point $B(p_1, p_2, p_3, p_4)$. If we call this curve α , then for every t inside the parameter interval I of α due to the implicit parametrisation of α , it is important to know the value $d(\alpha(t), p_4) = \rho(t)$, or in other words

$$f(\mathcal{O}_{p_4}(\rho(t), v_4(t))) = \alpha(t) \quad (30)$$

must hold as well as $\|v_4(t)\| = 1$ for all $t \in I$. Finally for the determination of the curve α introduce the system function

$$F(s, v_1, v_2, v_3) = \begin{pmatrix} \mathcal{O}_{p_1}(s, v_1) - \mathcal{O}_{p_3}(s, v_2) \\ \mathcal{O}_{p_1}(s, v_1) - \mathcal{O}_{p_3}(s, v_3) \\ \|v_1\|^2 - 1 \\ \|v_2\|^2 - 1 \\ \|v_3\|^2 - 1 \end{pmatrix}. \quad (31)$$

The integration of the trajectory $t \mapsto (s(t), v_1(t), v_2(t), v_3(t))$ can be stopped if for the radius function the condition $s(t) = \rho(t)$ holds. Remark that again the curve α has to be traced in both directions. It is convenient not to compute the distances $d(p_4, \alpha(t))$ in every step of the integration of the curve $B(p_1, p_2, p_3)$, since the update of the new distance $\rho(t + \Delta t)$ and the new direction $v_4(t + \Delta t)$ can be obtained by implicit differentiation of equation (30), similar to the integration process for the shortest geodesic connection problem. This part of the integration can be formulated separately but it makes more sense to reformulate the function F from (31). The local parametrisation of a face $B(p, q)$ for two sites $p, q \in S$ implicitly given by the zero set of $G(s, v_p, v_q) = \mathcal{O}_p(s, v_p) - \mathcal{O}_q(s, v_q)$ can be achieved with different approaches. One interesting approach is described in [EH99] which employs the normal form of an implicit parametrisation. It involves the second fundamental form of the implicit surface. We implemented a method that creates a

family of lines corresponding to isoparameters $v_p^i = \text{const}$ or $v_q^j = \text{const}$ which induces a local mesh of this face. However, the details are omitted here since it is similar to the computation of the curves $B(p, q, r)$ for three sites p, q, r .

A. Randomised incremental Construction of Voronoi Diagrams

Of course problems like the computation of the Euclidean Voronoi diagram are well understood and there exist some paradigms often used in computer science to treat them. These are mainly

- Divide and Conquer
- Incremental Construction
- Sweep

In fact, to the authors best knowledge there are no advances in computing Voronoi diagrams using the sweep algorithms in case of a metric not being equivalent to the Euclidean metric.

The sweep algorithm needs some explanations, even though we will not use it. Consider a discrete static geometrical problem in \mathbb{R}^d . We call this problem static since the prerequisites for the computations will not change during the sweep. The main idea is to transform the static d -dimensional problem into a dynamical $(d-1)$ -problem. There are several algorithms like the sweep line algorithm that treat the static structure of d -dimensional problems.

We will now focus on the structure of geodesic Voronoi diagrams for which we now that all sites are contained in a convex neighbourhood. Consider a graph manifold M and sites $p_i \in M, i = 1, \dots, n$. It will be convenient to identify the sites with the corresponding projections onto the parameter space \mathbb{R}^3 implying that the distance function is the induced distance function stemming from the first fundamental tensor (g_{ij}) of M . As in the Euclidean case the geodesic Voronoi diagram consists of **vertices**, **edges** and **faces**.

Definition 11: A face f is a maximal connected subset of $V(S)$ with the property that every $x \in f$ lies on exactly one bisector $B(p_i, p_j)$. A point v is called vertex if it lies on the boundary of k Voronoi regions for $k \geq 3$. An edge is a maximal connected subset of $V(S)$ enclosing all points that lie on the boundary of exactly two Voronoi regions

The most common way to describe the topology of Voronoi diagrams is **the Voronoi graph**. It corresponds to the skeleton of the Voronoi diagram is described below. The main topological information about the Voronoi diagram is contained in the vertices and the edges. Therefore, a greedy algorithm would be a first approach to determine the skeleton of the Voronoi diagram. It is highly recommended not to precompute the Voronoi vertices by verifying the circumsphere condition for any four points from S , since this has time complexity $O(n^5)$. There are $\binom{n}{4}$ possibilities for a circumsphere since every combination of four points may lead to such a sphere. If one has found such a sphere it has to be checked if no other point of the remaining $n-4$ points is contained in the inner of this sphere. Nevertheless it has been done for small n to prove the concepts of the last section.

Following the recommendations from [Le97] the complexity can be reduced in case $V(S)$ is a simple, abstract Voronoi diagram with specialised prerequisites. Therefore, we summarise the results from this paper. It must be emphasised that we did not implement this algorithm on a computer but ensuring that the convexity property can be fulfilled it will turn out that our local computational approaches serve well for the computation of the geodesic Voronoi diagram, using the randomised construction scheme. It will be shown that this incremental construction technique has time and space complexity $O(n^2)$. It is postulated that Voronoi regions have to be homeomorphic to a 3-ball or empty. In addition it is required that for given $p, q, r, s, t \in S$ the set $B(p, q) \cap B(q, r)$ is a transverse intersection of two bisectors. We will presume that this intersection only yields one component. The set $B(p, q) \cap B(q, r) \cap B(r, s)$ must be a point and $B(p, q) \cap B(q, r) \cap B(r, s) \cap B(s, t)$ must be empty. Finally, we will postulate that every circumsphere exactly contains 4 sites, which means that every vertex of the Voronoi diagram has outdegree 4. We will not admit big topological differences between the Euclidean and the geodesic Voronoi diagram. In this context it is required that inside a small neighbourhood of a vertex or a point of an edge the restriction of the Voronoi diagram to this neighbourhood looks topologically like a corresponding configuration in the Euclidean space (cf. figure 6).

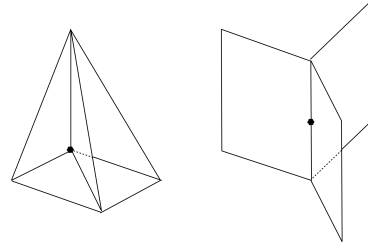


Fig. 6. Local behaviour of the Voronoi Diagram

All these prerequisites are necessary for the construction process of the simple Voronoi diagrams. They are mainly called simple because they must be topologically equivalent to Euclidean Voronoi diagrams. Although we did not present an axiomatic introduction like it was done in [Le97] the last notes shall be enough for the following considerations.

Definition 12: For a subset $R \subset S$ we define the respective sets $\text{Edge}(R)$ and $\text{Vert}(R)$, i.e. the set of edges and vertices of $V(R)$.

Definition 13: The skeleton of S is the set

$$\text{Skel}(S) = \text{Edge}(S) \cup \text{Vert}(S).$$

1) *The Algorithm:* From topological point of view the Voronoi diagram has its most important features (vertices) inside a sphere $\mathcal{S} = S(0, r)$ for a sufficiently large $r > 0$. It is required that this sphere intersects each $B(p_i, p_j)$ transversely. Moreover the union of all bisectors builds up a cell complex $C(S)$ for which we have the following property. Let $B(p_i, p_j)$ a bisector. Then the restriction of $C(S)$ to $B(p_i, p_j)$ outside

the domain of the sphere \mathcal{S} only consists of halflines and halfplanes.

We now add ∞ to the set of sites and define

$$\begin{aligned} B(p_i, \infty) &= B(\infty, p_i) = \mathcal{S}, \\ D(p_i, \infty) &= \{p \in \mathbb{R}^3; d_2(p_i, p) < r\}, \\ D(\infty, p_i) &= \{p \in \mathbb{R}^3; d_2(p_i, p) > r\}, \end{aligned}$$

where d_2 denotes the Euclidean metric.

The incremental construction process is based on some topological invariants. The skeleton of the Voronoi diagram carries the main topological features of $V(S)$. The first step therefore is to precompute the skeleton and determine the faces afterwards.

As in the Euclidean case we have the following important result for simple Voronoi diagrams

Lemma 1: The expected size of the structural complexity of the skeleton is at most $O(n)$, where n is the number of sites.

The proof of the lemma can be found in [DRA91].

The incremental construction involves an elementary operation that is assumed to have time complexity $O(1)$. Given five points $R = \{p, q, r, s, t\} \subset S$ assume $V(R)$ contains an edge e that starts at a vertex $B(p, q, r, s)$ and ends at a vertex $B(p, q, r, t)$. In addition a site $u \in S$ is introduced. Depending on if u is in **conflict** with the edge e , we have several possibilities for the structure of

$$e \cap \overline{VR(u, R \cup \{u\})}.$$

- 1) The intersection is empty, which means that there is no conflict.
- 2) The intersection is not empty, simply connected and contains
 - a) the entire edge.
 - b) the part of e that starts at $B(p, q, r, s)$.
 - c) the part of e that starts at $B(p, q, r, t)$.

Remark 1: e is in conflict with u , when the circumsphere of one of the endpoints of e (a vertex) contains the new point $u \in S \setminus R$.

The algorithm starts with the sites ∞, p_1, p_2, p_3 . The remaining sites are introduced step by step in a non deterministic order. This can be seen as an application of random sampling to on-line algorithms in computational geometry (cf. [BDS92]).

Definition 14: Let $e \in \text{Edge}(R)$. If e joins the points $B(p, q, r, s)$ and $B(q, r, s, t)$, then the **header** $D(e)$ of e is defined by:

$$D(e) = \{p, q, r, s, t\}.$$

Every edge e of a Voronoi diagram can be identified by its header $D(e)$.

Definition 15: Let e be an edge with header $D(e) = \{p, q, r, s, t\}$ and $u \in S \setminus \{p, q, r, s, t\}$. We say that u **intersects** with $D(e)$, if

$$e \cap VR(u, \{p, q, r, s, t, u\}) \neq \emptyset.$$

Several data structures are maintained during the construction process.

- Since we are only interested in the skeleton in the first instance, the Voronoi diagram can be represented as a **Levi graph** or **incidence graph** which is a bipartite graph. The black vertices of the Levi graph represent all elements of $\text{Vert}(R)$ and the white vertices symbolise analogue the elements of $\text{Edge}(R)$. There is an edge between a black and a white vertex if and only if their is a corresponding incidence between a Voronoi vertex and a Voronoi edge.
- The history graph $\mathcal{H}(R)$ contains all edges that appeared during the construction process. It is a **directed acyclic graph** (DAG) with a source Q that does not contain any information about the edges.

There are three invariant properties of $\mathcal{H}(R)$:

- The leaves of $\mathcal{H}(R)$ correspond to the actual Voronoi edges of $V(R)$. They do not have outgoing edges, whereas every vertex of $\mathcal{H}(R)$ can not have more than four outgoing edges.
- The header of an edge $e \in \text{Edge}(R)$ is attached to all vertices. It contains the information of all Voronoi vertices that are involved in the genesis of e , for example the points p, q, r, s, t from above.
- When a new site u is introduced, there may be leaves that are in conflict with u . For each of these leaves, e.g. D , there exists a path from Q to D that is only incident to vertices that intersect with u .

For a new site u all intersecting edges $E(u)$ need to be detected. This can be achieved quickly using the history graph $\mathcal{H}(R)$.

Lemma 2: The time complexity of finding $E(u)$ lies in $O(|A|)$, where A denotes the set of intersecting vertices $v \in \mathcal{H}(R)$.

The proof of this theorem uses mainly the invariance properties.

The update mechanism for the simple Voronoi diagram and the history graph are based on some relevant topological properties and some easy combinatorial results. Note that some Voronoi vertices are deleted in the next step whereas some new vertices will come into play. In particular if a vertex v lies outside the new Voronoi region $U = VR(u, R \cup \{u\})$ it stays in the vertex list.

If e is an intersecting edge, i.e. $e \in E(u)$, then new vertices v have to be introduced which correspond to the intersection points. We will denote this by $v \in V_{\text{new}}$. Let $x \in \text{Vert}(R)$ be an old vertex and e be an outgoing Voronoi edge that has to be shortened. If the piece of the intersected edge that becomes part of the new edge list $\text{Edge}(R \cup \{u\})$ is incident to x then x stays in the list, if it is true for every outgoing edge. We will denote this by $x \in V_{\text{unchanged}}$. It can be shown that only these types of points contribute to the new vertex list $\text{Vertex}(V \cup \{u\})$.

The new question that arises is now how long the construction of $V(R \cup \{u\})$ takes. In fact, the time complexity

is bounded by the number of conflicting edge. The major effort lies in the identification of the edges of the new faces f resulting from the introduction of the new site u .

We will try to make this more lucid by an two-dimensional example (cf. figure 7). Consider for example the edge w_5 that has to be constructed. It joins the points q_1 and q_2 that are both elements of V_{new} . If we start from q_1 than q_2 can be found by following the boundary segments from Voronoi region $VR(p_1, \{p_1, p_2, p_3, p_4, p_5\})$. The red arrow indicates the first segment, whereas the green and blue arrows indicate the sequent segments. This procedure must be iterated until all boundary segments of the new region $VR(p_6, \{p_1, p_2, p_3, p_4, p_5, p_6\})$ are found. These segments build a loop.

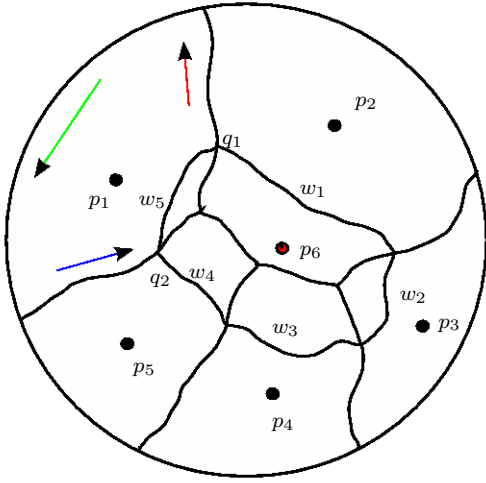


Fig. 7. Construction of the new Voronoi region

It can be shown that updating the history graph has the same time complexity as the prescribed construction of $V(R \cup \{u\})$. The subsequent steps are necessary for a correct update.

- The edge $e \in \text{Edge}(R \cup \{u\})$ is the son of an edge $e' \in \text{Edge}(R)$, if e is shortened and $e \subset e'$.
- For every new edge e add the edges (e', e) to the history graph for all edges e' that were found during the construction of the endpoints of the new segment (in the example these were the edges being identified by the coloured arrows for the new edge w_1).

One can show that no invariance property is harmed by the former construction process. [BDS92] provides the expected values for time and space in relation to the total expenditure. Both values lie in $O(n^2)$ with n the number of sites.

The results below give some examples of some simple Voronoi diagram containing only few sites.

V. RESULTS

The examples given within this section are rather simple. More sites automatically lead to an arrangements of faces and edges that would overstrain the reader. Hence in the first case

the manifold is parametrized by the map

$$f(x, y, z) = \begin{pmatrix} x \\ y \\ z \\ x^2 + y^2 + z^2 \end{pmatrix} \quad (32)$$

The coordinates of the sites with respect to the map f are given through $(0, 0, 0)$, $(1, 0, 0)$, $(\frac{1}{2}, \frac{\sqrt{3}}{2}, 0)$ and $(\frac{1}{2}, 1 - \frac{1}{\sqrt{3}}, \sqrt{\frac{2}{3}})$. In fact these site are the vertices of a regular tetrahedron. In the second case the manifold is parametrized by the map

$$f(x, y, z) = \begin{pmatrix} x \\ y \\ z \\ \frac{1}{2}(x^2 - yz) \end{pmatrix} \quad (33)$$

The coordinates of the sites with respect to the map f are given through $(0, 0, 0)$, $(0.8, 0, 0)$, $(0.9, 1.1, 0)$, $(1, 1.5, 1)$ and $(0, 1.14, 0.98)$.

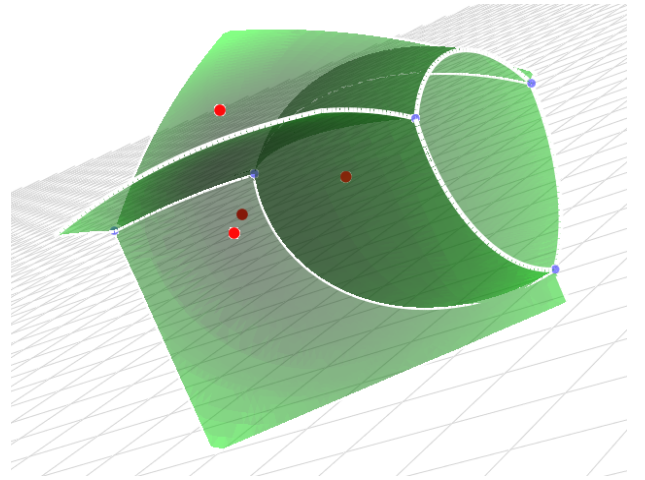


Fig. 8. Voronoi Diagram of four sites

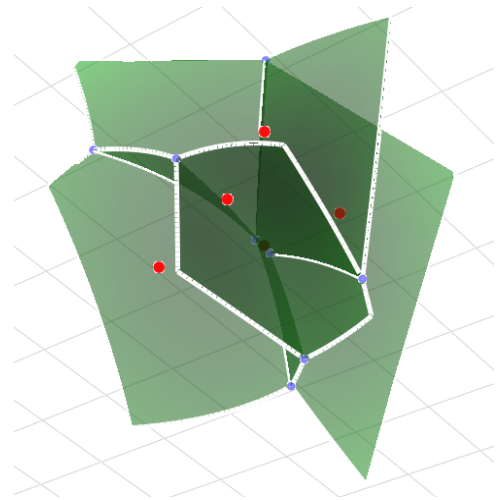


Fig. 9. Voronoi Diagram of five sites

VI. CONCLUSION

This work gives an overview of some newest results concerning the geodesic Voronoi diagram computation on Riemannian manifolds M . Our approach uses the normal coordinates (or geodesic polar coordinates) for the local description of the so called faces, the edges and the vertices of a Voronoi diagram that has basically the same topological properties as the Euclidean Voronoi diagram. For the incremental computation of the Voronoi diagram $V(S)$ it is convenient to focus only on the skeleton of the Voronoi diagram consisting of all edges and vertices. This computation begins with an initial situation of five sites $R = \{p_1, \dots, p_5\}$ including the site ∞ . One major effort of the computations basically lies in the determination of this initial diagram, since it requires the localisation of the first vertex of $V(R)$. The localisation of the vertex involves a perturbation method for an accurate determination of minimal joins of two sites in order to detect an initial bisector point of the two sites that yields the starting point of a piecewise differentiable curve joining the bisector point and the vertex.

The RICS that was originally presented in [Le97] requires time and space complexity $O(n^2)$, where n denotes the number of sites. It uses a Levi graph and a DAG for its implementation. We showed how the requirements of this algorithm can be achieved and we gave some example for the proof that this method can be extended beyond the scope of [Le97].

Future works on this subject will focus on the global phenomena concerning the injectivity of the exponential map in order to understand the main differences between Euclidean and non Euclidean Voronoi diagrams.

ACKNOWLEDGMENT

This paper presents major parts of four years of PhD thesis research of the first author at the Leibniz Universität Hannover. This research was made possible by a scholarship of the Graduiertenkolleg 615 (GRK 615) financed by the Deutsche Forschungsgemeinschaft. The first author H. Naß thanks Prof. E. Stephan being the speaker GRK 615 for granting him this scholarship and he wants to thank Prof. Stephan's staff for their warm welcome to the GRK 615. Finally H. Naß wants to thank Prof. Patrikalakis for inviting him to a four month research visit at MIT in 2006 a period during which important results of the PhD. thesis project were accomplished.

REFERENCES

- [Wol92] Wolter F.-E., *Cut Locus & Medial Axis in Global Shape Interrogation & Representation*, MIT Design Laboratory Memorandum 92-2 and MIT Sea Grant Report, 1993
- [Boe04] Guido Bötcher, *Medial Axis and Haptics*, Leibniz university of Hannover, October
- [LL92] Leymarie, F., and Levine, M.D., *Simulation of the Grassfire Transform using an active Contour Model*, IEEE Trans. Patt. Anal. Machine Intell., 14, 1, pp. 56-75, 1992
- [Set99] Sethian, J.A., *Level Set Methods and Fast Marching Methods, Evolving Interfaces in Computational Geometry, Fluid Mechanics, Computer Vision, and Material Science*, Cambridge University Press, second ed., 1999
- [RWS97] T. Rausch, F.-E. Wolter, O. Sniehotta, *Computation of Medial Curves on Surfaces*. In T. Goodman and R. Martin, editors, *The Mathematics of Surfaces VII*, pages 43-86. Information Geometers 1997.

- [Vor07] Georgy Voronoi *Nouvelles applications des paramtres continus la theorie des formes quadratiques*, Journal für die Reine und Angewandte Mathematik, 133:97-178, 1907
- [OBS00] Okabe A., Boots B., Sugihara K., *Spatial Tessellations: Concepts and Applications of Voronoi Diagrams*, 2nd ed. New York: Wiley, 2000.
- [Bee75] John K. Beem, *Pseudo-Riemannian Manifolds with Totally Geodesic Bisectors*, Proceedings of the American Mathematical Society, Volume 49, Number 1, May 1975
- [Wol85] F.-E. Wolter, *Cut Loci in Bordered and Unbordered Riemannian Manifolds*, Dissertation, Berlin 1985
- [Ede87] H. Edelsbrunner, *Algorithms in Combinatorial Geometry*, volume 10 of *EATCS Monographs on Theoretical Computer Science*. Springer, Heidelberg, 1987
- [doC98] Manfredo Perdiago do Carmo, *Differentialgeometrie von Kurven und Flächen*, Vieweg Verlagsgesellschaft, 3. Auflage, 1998
- [Le97] Ngoc-Minh Lê, *Randomized incremental construction of simple abstract Voronoi diagrams in 3-space*, Computational Geometry 8 (1997), 279-298
- [BDS92] Jean-Daniel Boissonat, Olivier Devillers, Rene Schott, Monique Teillaud, Mariette Yvinec, *Applications of Random Sampling to On-Line Algorithms in Computational Geometry*, Discrete and Computational Geometry 8, 51-71, 1992
- [Gra04] Alfred Gray, *Tubes*, Progress in Mathematics, sec. ed. Birkhäuser, 2004
- [PM02] Nicholas M. Patrikalakis, Takashi Maekawa *Shape Interrogation for Computer Aided Design and Manufacturing*, Springer, Berlin, 1. Edition, 2002
- [SPW96] E. Sherbrooke, N. M. Patrikalakis, F.-E. Wolter, *Differential and Topological Properties of Medial Axis Transforms*, Graphical Models and Image Processing, Vol. 58, No. 6, pp. 574-592, Nov. 1996.
- [KWR97] R. Kunze, F.-E. Wolter, T. Rausch, *Geodesic Voronoi Diagrams on Parametric Surfaces*, Published in: CGI '97, IEEE, Computer Society Press Conference Proceedings, pp. 230-237, June 1997.
- [Eul52] L. Euler, *Elementa doctrinae solidorum – Demonstratio nonnullarum insignium proprietatum, quibus solida hedris planis inclusa sunt praedita*, Novi comment acad. sc. imp. Petropol., 4, 1752-3, 109-140-160.
- [Poi95] H. Poincaré, *Analysis Situs*, Jour. cole Polytechnique 2, 1 (1895).
- [HT07] Hannes Thielhelm, *Geodätische Voronoi Diagramme*, Diploma thesis, Leibniz Universität Hannover, 2007
- [TR99] Thomas Rausch *Analysis and Computation of the Geodesic Medial Axis of Bordered Surface Patches*, Leibniz Universität Hannover, 1999.
- [DRA91] R. A. Dwyer, *Higher dimensional Voronoi diagrams in linear expected time*, Discrete Comp. Geom., 6:343-367, 1991
- [EH99] Erich Hartmann, *Numerical parametrisation of curves and surfaces*, Computer Aided Geometric Design 17 (2000) 251-266
- [doC92] Manfredo Perdiago do Carmo, *Riemannian Geometry*. Mathematics: Theory and Applications, Birkhäuser Verlag, Boston, 1992